Electronic Journal of Biotechnology 66 (2023) 1–16

Contents lists available at ScienceDirect

Electronic Journal of Biotechnology

journal homepage: www.elsevier.com/locate/ejbt

Research Article

Heterologous expression and characterization of a *Mo*AA16 polysaccharide monooxygenase from the rice blast fungus *Magnaporthe oryzae*

Hung M. Nguyen [a,*], Loan Q. Le [b,c,d], Luca Sella [e], Luke M. Broadbent [f], Roslyn M. Bill [f], Van V. Vu [d,*]

[a] *Center for Pharmaceutical Biotechnology, College of Medicine and Pharmacy, Duy Tan University, Da Nang 55000, Viet Nam*
[b] *Institute of Tropical Biology, Vietnam Academy of Science and Technology, Viet Nam*
[c] *University of Science, Vietnam National University, Ho Chi Minh City, Viet Nam*
[d] *NTT Hi-Tech Institute, Nguyen Tat Thanh University, 298-300A Nguyen Tat Thanh Street, District 4, Ho Chi Minh City, Viet Nam*
[e] *Department of Land, Environment, Agriculture and Forestry, University of Padova, viale dell'Università 16, 35020 Legnaro, Italy*
[f] *College of Health & Life Sciences, Aston University, Aston Triangle, Birmingham B4 7ET, United Kingdom*

GRAPHICAL ABSTRACT

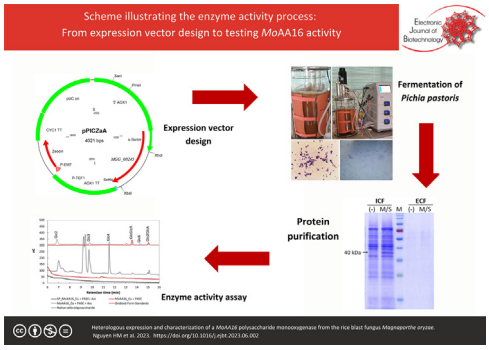

ARTICLE INFO

Article history:
Received 6 April 2023
Accepted 28 June 2023
Available online 18 August 2023

Keywords:
Cellulose
Enzymatic activity
Fungal infection
Heterologous expression
Magnaporthe oryzae
Monosaccharide
Oxidative cleavage
Pichia pastoris

ABSTRACT

Background: Cellulose is an organic carbon source that can be used as a sustainable alternative for energy, materials, and chemicals. However, the substantial challenge of converting it into soluble sugars remains a major obstacle in its use as a biofuel and chemical feedstock. A new class of enzymes knowns as copper-dependent polysaccharide monooxygenases (PMOs) or lytic polysaccharide monooxygenases (LPMOs) can break down polysaccharides such as cellulose, chitin, and starch through oxidation. This process enhances the efficiency of cellulose degradation by cellulase.
Results: The genome of the fungus *Magnaporthe oryzae*, the causal agent of rice blast disease, contains the *MGG_00245* gene, which encodes a putative PMO referred to as *Mo*AA16. *Mo*AA16 has been found to be highly expressed in planta during the early stages of fungal infection. The gene was optimized for heterologous expression in *Pichia pastoris,* and its oxidative cleavage activity on cellulose was characterized by analyzing soluble oligosaccharide products using highperformance anion exchange chromatography (HPAEC-PAD). The reaction catalyzed by *Mo*AA16 requires 2 electrons from an electron donor, such as

Abbreviations: BMGY, Buffered glycerol-complex medium; BMMY, Buffered methanol-complex medium; HRP, Horseradish peroxidase substrate; LB, Lysogeny broth; MCS, Multiple cloning sites; MWCO, Molecular weight cutoff; Ni-NTA, Nickel 2+ ion that has been coupled to Nitrilotriacetat acid (NTA); PBST, Phosphate buffered saline – tween; YPD, Yeast extract peptone dextrose.

Peer review under responsibility of Pontificia Universidad Católica de Valparaíso

* Corresponding authors.
E-mail addresses: hungmolbio@gmail.com (H.M. Nguyen), anhvan.vu@gmail.com (V.V. Vu).

https://doi.org/10.1016/j.ejbt.2023.06.002

Polysaccharide monooxygenase
Protein expression
Rice blast fungus

ascorbic acid, and aerobic conditions. It primarily produces Glc1 to Glc4 oligosaccharides, as well as oxidized cellobionic and cellotrionic acids. *Mo*AA16 has been observed to enhance cellulase hydrolysis on phosphoric acid swollen cellulose (PASC) substrate, resulting in the production of more monosaccharide products.

Conclusions: Our findings reveal the successful heterologous expression of *Mo*AA16 in *P. pastoris* and its cellulose-active PMO properties. These results highlight the potential of *Mo*AA16 as a promising candidate for applications in biofuel production and chemical synthesis.

How to cite: Nguyen HM, Le LQ, Sella L, et al. Heterologous expression and characterization of a *Mo*AA16 polysaccharide monooxygenase from the rice blast fungus *Magnaporthe oryzae*. Electron J Biotechnol 2023. https://doi.org/10.1016/j.ejbt.2023.06.002.

1. Introduction

Cellulose, the most abundant organic carbon source on Earth, has the potential to serve as a sustainable alternative source of energy, materials and chemicals [1]. However, its extreme recalcitrance in conversion into soluble sugars poses a significant technological bottleneck, hindering its cost-effective use as a feedstock for biofuel and chemical production [2]. In order to degrade major structural polysaccharides like cellulose found in the plant cell wall, microbes produce a variety of cell wall-degrading enzymes. The complete hydrolysis of cellulose requires the action of three main types of cellulose-hydrolytic enzymes. Endo-β-1,4-glucanases randomly attack the internal bonds of cellulose chains, resulting in the production of cellulose oligomers. Cellobiohydrolases, on the other hand, attack cellulose from either the reducing- or non-reducing-ends, producing cellobiose, a disaccharide composed of glucose. Finally, β-glucosidases or cellobiases hydrolyze cellobiose into glucose, which can be readily absorbed and metabolized by microorganisms.

Recently, a series of studies have identified a novel class of carbohydrate-active enzymes called CAZymes that play a central role in breaking down polysaccharides such as chitin [3,4,5], cellulose [3,5], and starch [6,7] using an oxidative mechanism. These enzymes are described as Cu^{2+}-dependent polysaccharide monooxygenases (PMOs) due to their oxidative mode of action and dependence on copper ions (Cu^{2+}) as co-factors [8]. PMOs are also known as lytic polysaccharide monooxygenases (LPMOs) and they work in synergy with cellobiose hydrolases and other cellulolytic enzymes to significantly enhance the enzymatic degradation of cellulose [2,4,8,9,10,11]. Indeed, several studies have reported that the addition of a small amount of PMO (1-5%) to the typical hydrolytic cellulase mixture greatly improved cellulolytic activity, resulting in a 3-5 times more efficient conversion of cellulose to fermentable sugars [12].

In the CAZy database, PMOs are classified as auxiliary activity (AA) enzymes. Currently, PMOs are divided into six families based on their amino acid sequence similarities and substrates [13]: (i) cellulose-active fungal PMOs [8,11,12,14] (AA9, formerly classified in the glycoside hydrolase family GH61, and AA16); (ii) chitin- and/or cellulose-active bacterial PMOs [3,4,5] (CBM33 or AA10); (iii) chitin-active fungal PMOs (AA11) [3,4,5]; (iv) starch-specific fungal PMOs (AA13) [6,7]; (v) xylan-active fungal PMOs (AA14), which act on xylan coating cellulose fibers [15]; (vi) cellulose and chitin-active PMOs (AA15) of animal origin [16].

PMOs are secreted by various strains of filamentous fungi and bacteria [3,17,18,19,20]. Among fungi, several plant pathogens secrete PMOs during plant infection, including rusts, powdery mildews, and *Magnaporthe oryzae* (teleomorph of *Pyricularia oryzae*). *M. oryzae* is the causal agent of rice blast disease, which is highly prevalent in temperate rice-growing regions [21] and leads to a 30% reduction in total annual rice production [22]. During the early stages of the pathogenic process, this fungus develops a pressurized dome-shaped melanin-pigmented cell known as an appressorium. This fungal cell generates an enormous cellular turgor pressure (up to 8 MPa), physically breaking the leaf cuticle to facilitate fungal penetration into plant tissues [23,24,25]. Appressorium formation has been extensively studied using molecular biological methods [25,26,27]. Genome-wide transcriptional profiling has revealed high expression of many putative carbohydrate-active enzymes during appressorium development [25,26]. Among these enzymes, we have identified a putative *M. oryzae* PMO (*Mo*AA16) belonging to the AA16 family that may play a role in appressorium development.

*Aa*AA16 from *Aspergillus aculeatus*, the first member of the PMO AA16 family, has demonstrated activity on cellulose with oxidative cleavage at the C1 position of the glucose unit [1]. It has also been revealed to enhance catalytic efficiency when co-working with *Trichoderma reesei* cellulase CBHI on cellulosic substrates. Additionally, the oxidase activity of *Mt*AA16A from *Myceliophthora thermophila* and *An*AA16A from *Aspergillus nidulans* significantly enhanced the degradation of cellulose by four AA9 PMOs from *M. thermophila* (*Mt*PMO9s) [28].

Currently, the CAZy database contains approximately 68 homologous sequences annotated in the AA16 family, most of which are found in many important pathogenic fungi. In a recent study, an analysis of 27,060 PMO sequences revealed that 60% of them have a C-terminal extension predicted to be disordered. Furthermore, the analysis showed that 80% of the sequences with unknown function (UNK) in PMO families AA9, AA14, and AA16 are expected to have at least one Long Disordered Region (LDR). These extensions, which are unique to PMOs, have variable lengths and compositions and may undergo post-translational modifications. The presence of these extensions in PMOs from diverse organisms suggests that they may have a functional role, presenting new research opportunities [29].

This study focuses on the cloning, heterologous expression in the methylotropic yeast *Pichia pastoris*, and purification of *Mo*AA16. The aim is to characterize the enzymatic activity of recombinant *Mo*AA16, verifying its possible role in fungal pathogenesis and its application in an efficient and cost-effective process for converting cellulose into soluble sugars. The purified recombinant *Mo*AA16 was found to enhance the degradation of phosphoric acid swollen cellulose (PASC), indicating that this cellulose-active enzyme possesses oxidative cleavage and depolymerizing activity. These findings are crucial for the development of sustainable sources of energy, materials and chemicals.

2. Methods

2.1. Chemicals and microorganisms

All chemicals were sourced from Sigma-Aldrich, Fermentas, Invitrogen, Thermo Scientific or Qiagen at the highest purity, unless specified otherwise. Subcloning was performed using the *E. coli* strain DH5α from Invitrogen. The *P. pastoris* strain X-33 and the pPICZαA vector are components of the Pichia Easy Select Expression System from Invitrogen.

2.2. Identification of the MoAA16

The *MGG_00245* gene, which encodes *Mo*AA16, was identified by analyzing a published dataset on genome-wide transcriptional profiling of appressorium development in *Magnaporthe oryzae* [25]. The nucleotide and amino acid sequences of *Mo*AA16 were retrieved from NCBI (http://www.ncbi.nlm.nih.gov) and UNIPROT (https://www.uniprot.org/), respectively. The amino acid sequence of MoAA16 was analyzed using the Hidden Markov Model (HMM) provided by the European Molecular Biology Laboratory (EMBL), including HMMer (https://www.ebi.ac.uk/Tools/hmmer/) and SMART domain prediction (http://smart.embl-heidelberg.de/). An iterative HMM search was performed to identify homologs of *Mo*AA16 in other organisms.

2.3. Codon Optimization and Synthesis of the Gene

The codon usage of the *MGG_00245* gene (from GenBank) was analyzed using GeneScript (genscript.com) and optimized by replacing codons predicted to be less frequently used in *P. pastoris*. The *Mo*AA16 signal peptide was analyzed using SignalP (http://www.cbs.dtu.dk/services/SignalP). The optimized gene was synthesized by GeneScript, USA (Fig. S1, Fig. S2, Fig. S3, Fig. S4).

2.4. PCR amplification of the MGG_00245 gene

Two primers, *MGG_00245* -F1: 5'-TACTCGAG**AAAAGA**CACGGTAATATCACTGTCC-3' and *MGG_00245* -R: 5'-ATTCTAGAATACCCTGGACGAAATCGACA-3' (*Xho*I and *Xba*I sites underlined, respectively; kex2 cleavage site in bold), were designed to amplify the *MGG_00245* gene in a 50 μL PCR reaction mixture. The reaction contained DreamTaq PCR Master Mix (2x) (ThermoScientific, K1071), 0.5 mM of each primer, and 50 ng of the *MGG_00245* plasmid, (synthesized by Genescript) as the template. The PCR program consisted of an initial denaturation at 95°C for 30 s, followed by 30 cycles of denaturation at 95°C for 30 s, annealing at 58°C for 30 s, extension at 72°C for 60 s, and a final extension at 72°C for 5 min. The PCR product was analyzed using 1% (w/v) agarose gel electrophoresis (BioBasic, D0012) and visualized with Red-Safe Solution (iNtRON, 21141) on a Blue LED Illuminator. The desired ~518 bp band was purified using the QIAquick Gel Extraction Kit (Qiagen, 28706).

2.5. Cloning of the MGG_00245 gene into pPICZαA

2.5.1. Enzymatic digestion and ligation

The purified *MGG_00245* gene and the pPICZαA vector (TFS, V19520) were digested using *Xho*I and *Xba*I (NEB, R0145S and R0142S, respectively), then purified with the QIAquick PCR Purification Kit (Qiagen, 28106) following the manufacturer's instructions. Subsequently, the digested *MGG_00245* gene was ligated into the linearized pPICZαA vector in frame with the His tag using T4 DNA ligase (NEB, M0202S) in a 20 μL reaction (2 μL 10× Rapid Ligation Buffer, 10 μL DNA (~100 ng), 1 μL 5 U/μL T4 DNA ligase) incubated at 22°C for 2 h.

2.5.2. Transformation and screening of E. coli

For the transformation of competent *E. coli* DH5α cells (Invitrogen), 10 μL of the ligation mixture was used and subjected to heat shock at 42°C for 30 s. The transformed cells were then recovered by adding 500 μL of liquid LB medium and incubating them at 37°C for 1 h. Subsequently, the cells were plated on LB plates supplemented with 25 μg/mL Zeocin (TFS, R25001). After an overnight incubation at 37°C, ten colonies were selected and cultured in 3 mL liquid LB medium supplemented with 25 μg/mL Zeocin at 37°C. The recombinant plasmids were extracted from the cell pellets using the GeneJET Plasmid Miniprep kit (TFS, K0503) following the manufacturer's instructions. Screening of the recombinant plasmids was performed by *Xho*I and *Xba*I digestion of the *MGG_00245* gene.

2.6. Sequencing and analysis

Positive clones were confirmed by sequencing the purified plasmid using the ABI Prism BigDye terminator cycle sequencing kit along with the *AOX1* promoter (5'AOX-F: 5'-GACTGGTTCCAATTGACAAGC-3') and terminator (3'AOX1-R: 5'-GCAAATGGCATTCTGACATCC-3') primers. The consensus sequences were generated by aligning both strands and validated using DNAstar software V7.

2.7. Small-scale expression of recombinant MoAA16

2.7.1. Plasmid preparation

One positive colony of *E. coli* was cultured overnight at 37°C in 50 mL liquid LB medium supplemented with 25 μg/mL Zeocin. The recombinant plasmid (pPICAαA-*MGG_00245*) was isolated using the GenElute Plasmid Midiprep kit (Sigma-Aldrich, NA0200) according to the manufacturer's instructions and linearized with *Pme*I (NEB, R0560S). The linearized plasmid was then separated on a 1.5% agarose gel and purified using the Wizard SV Gel and PCR Clean-Up System (Promega, A9281) following the manufacturer's instructions.

2.7.2. Transformation

A total of 5 μg of the linearized recombinant vector was transformed into 50 μL of competent *P. pastoris* X33 cells using a Genepulser electroporator (Bio-Rad) at 1,800 V, 25 μF, and 600 Ω in a 10 mm gap electroporator cuvette. The cells were then recovered by adding 1 mL of 1 M ice-cold sorbitol and incubating at 30°C for 2 h. One hundred μL of the transformed mixture was then plated on YDPS plates supplemented with Zeocin at concentrations of 100, 200, and 500 μg/mL, and incubated at 30°C for 2–3 d until colonies appeared.

2.7.3. Small-scale induction

For expression screening, 24 transformed colonies were grown in 2.5 mL of BMGY media without Zeocin at 30°C in a Corning Micro-24 plate until reaching an OD_{600} of 15–20. The cells were then centrifuged and transferred to 10 mL of BMMY-inducing medium. Every 24 h post-induction, cells and culture media were harvested, and 1% methanol was added (a total of 72 h of induction).

2.7.4. Secreted protein preparation

Cultures were centrifuged at 5,000 rpm for 3 min, and 20 μL of the supernatant was collected for immunoblot analysis.

2.7.5. Intracellular protein preparation

Cell pellets were used to determine the total intracellular protein. To the cell pellets, 1 mL of breaking buffer (50 mM Na_2HPO_4,

50 mM NaH_2PO_4, 2.0 mM EDTA, 100 mM NaCl, 5% glycerol; pH 7.4), 2.0 μL of protease inhibitor (Calbiochem), and 200 mg of glass beads were added. The cells were then lysed by vortexing at 50 Hz for 3 min using a Tissue Lyser LT (Qiagen). The supernatant was transferred to a 1.5 mL Eppendorf tube and centrifuged at 13,000 rpm for 15 min. The resulting cell lysate was used for immunoblot analysis.

2.7.6. Immunoblot

To detect the His_6-tag fused to the *Mo*AA16 protein in the supernatant (culture medium) or intracellular protein (cell lysate), immunoblotting was used. Samples (20 μL) and a Protomarker prestained protein ladder (5 μL) (National Diagnostics) (10–225 kDa) were applied to a 12.5% SDS gel and run in 1×Tris/glycine/SDS (GeneFlow) at 100 V for 1 h. The SDS gel was then transferred to a nitrocellulose membrane (Whatman, 09-301-111), blocked in 5% milk in 1 × PBS buffer, and incubated with primary antibody (6 × His monoclonal antibody, Serotec) at a 1:5,000 dilution at room temperature for 1 h. After washing with 1 × PBST, the membrane was incubated with a secondary antibody against mouse IgG conjugated with HRP (Sigma, A0545) at a 1:5,000 dilution for 1 h. After washing with 1 × PBST, the protein bands on the membrane were detected using EZ-ECL chemiluminescence solution (GeneFlow, 20-500-120) and visualized with a Uvitec instrument.

2.8. Large-scale expression of recombinant MoAA16

The positive *P. pastoris* pPICZαA-*MGG_00245* strain was cultured on a YPD agar plate supplemented with 100 μg/mL Zeocin and incubated at 30°C for 48 h. Cell culture was initiated by transferring a single colony into 25 mL of YPD medium with 100 μg/mL Zeocin and incubating it in a shaking incubator at 30°C and 150 rpm. The first-stage culture was prepared by transferring the cell culture to 400 mL of BMGY media without Zeocin and incubating it at 30°C and 150 rpm until reaching an OD_{600} of 1-2. Fermentation was performed by transferring the first-stage culture to a 5 L BioFlo 120 bioreactor containing BMGY medium at pH 6.0. The culture was agitated at 30°C, 250 rpm, with an air flow rate of 10 L/min, and dissolved oxygen (DO) was continuously monitored. The glycerol batch phase was extended until the DO reached 0, followed by a fed-batch phase with 50% glycerol at a rate of 3.65 mL/h/L. The methanol/sorbitol fed-batch phase involved continuously adding 100% methanol supplemented with 12 mL/L PTM1 salt solution (pump 1) and 50 g/L sorbitol (pump 2) at a rate of 3.65 mL/h/L for 6 h. This was followed by an increase to 7.3 mL/h/L for the next 6 h and finally to 10.9 mL/h/L until induction was complete (approximately 48 h). Samples were taken to track wet cell weight (WCW) and total protein concentration.

2.9. Recombinant protein purification

2.9.1. Separation and harvest of the recombinant protein

The target protein was collected from both the extracellular fluid (ECF) and intracellular fluid (ICF). ECF was collected by centrifuging at 4000 rpm for 15 min, filtered, and concentrated using a Pellicon 2 cassette filter system with a 10 kDa filter. The ECF containing proteins larger than 10 kDa was stored at 4°C for protein purification. The ICF was mixed with NPI-10 lysis buffer (50 mM NaH_2PO_4, 300 mM NaCl, 10 mM Imidazole) and 1X protease inhibitors. Then, the cells were lysed by ultrasonic waves at 400 W, with 60 cycles of 5 s of lysis and 10 s of pauses. The ICF proteins were collected by centrifuging at 4000 rpm for 15 min.

2.9.2. Target protein purification

The target protein in ECF and ICF was purified using Ni-NTA affinity chromatography (Qiagen). The Ni-NTA column was equilibrated with NPI-10 buffer (Qiagen), and protein solutions were run through the column at a flow rate of 1 mL/min. The column was washed with NPI-20 (Qiagen), and the target protein was eluted with increasing imidazole concentrations (30 to 250 mM). The eluted fractions were analyzed by SDS-PAGE, recombined on a PD miniTrap G-25 column, and desalted with 50 mM Tris-HCl, pH 8.0. For ICF, the α-factor was cleaved by Kex2 protease. The reaction was performed in Tris-HCl pH 8.0 by adding Kex2 protease to the protein solution at a mass ratio of 1:50 and incubating the mixture at 37°C for 16 h. The target protein was then concentrated using a Vivaspin 10 kDa MWCO filter column and verified by SDS-PAGE gel and ImageJ software. The Bradford Protein Assay was used to estimate the protein concentration by mixing the protein solution with the Bradford reagent and measuring the absorbance at 595 nm. The absorbance reading was used in conjunction with a standard curve generated using BSA to calculate the protein concentration.

2.10. Enzyme activity

2.10.1. Reconstitution of copper

Copper reconstitution of *Mo*AA16 was performed to coordinate Cu(II) ions with its active site. The purified *Mo*AA16 solution was treated with 100 mM EDTA to remove metal ions, and then, excess EDTA was removed by buffer exchange using a HiTrap G-25 column. A 10-fold excess of $CuSO_4$ was slowly added to the desalted protein solution and incubated at room temperature for 1–2 h. The protein solution was purified using a HiPrep 26/10 column and dialyzed. The final product, Cu(II)-reconstituted *Mo*AA16, was used in the enzyme activity assay.

2.10.2. Preparation of phosphoric acid swollen cellulose (PASC)

A quantity of 0.2 g of Avicel (microcrystalline cellulose) was thoroughly mixed with 500 μL of distilled water. Subsequently, 10 mL of 85% H_3PO_4 solution was gradually added while continuously stirring until the solution became transparent. After incubating for 1 h on ice, stirring occasionally, 40 mL of cold water was gradually added to the solution while vigorously stirring until a white precipitate formed. The solution was then centrifuged 4 times at 5000 g for 20 min at 4°C to obtain a precipitate. To neutralize the solution, 500 μM of 2 M Na_2CO_3 was added, followed by repeated washing with 45 mL of cold water and subsequent centrifugation. Finally, 100 mM acetate buffer (pH 5.0) and sodium azide were added, and the substrate was stored at 4°C.

2.10.3. MoAA16 treatment

The enzyme reaction was performed by mixing 50 mg of PASC substrate, 2 mM ascorbic acid, 0.6 μM Cu(II)-reconstituted *Mo*AA16, and acetate buffer to make a final volume of 1 mL. The control reaction was conducted by replacing the *Mo*AA16 protein with acetate buffer. The reaction was carried out at a pH of 5.0 and a temperature of 40°C for 16 h and was stopped by adding NaOH to a final concentration of 0.2 M. The reaction products (soluble and insoluble oligosaccharides) were recovered by centrifugation at 10,000 *g* for 15 min.

2.10.4. Cellulase treatment of MoAA16 reaction products

Cellulase is commonly used to break down cellulose into fermentable sugars. PMO treatment can enhance the accessibility of the cellulose substrate for cellulases, resulting in an increased rate and yield of glucose production. Following the *Mo*AA16 treatment, 1 U of cellulase (Megazym) was incubated with the *Mo*AA16 reaction products, which included both soluble and insoluble oligosaccharides, at 42°C for 8 h. The reaction was then deactivated at 80°C. The resulting products were analyzed using high-performance

anion exchange chromatography with an amperometric detector (HPAEC-PAD).

2.10.5. Combined treatment with MoAA16 and cellulase

A combined treatment with *Mo*AA16 and cellulase was performed by adding 50 mg of PASC substrate, 2 mM ascorbic acid, 0.6 μM Cu(II)-reconstituted *Mo*AA16, and 1 U of cellulase. A control reaction without cellulase was also prepared. The reaction was maintained at 40°C, and samples were collected at various time intervals: 0 min, 5 min, 10 min, 15 min, 20 min, 30 min, 1 h, 2 h, 3 h, 4 h, 6 h, 8 h, 10 h, and 12 h. After the final time point, the reaction was stopped by adding NaOH to a final concentration of 0.2 M. Oligosaccharides were retrieved by centrifugation at 10,000 *g* for 15 min.

2.10.6. Detection of the resulting oligosaccharides using HPAEC-PAD

The obtained oligosaccharides were analyzed using the Dionex ICS-3000 HPAEC-PAD system. The PA-200 HPAEC column was eluted with a gradient of 0.1 M NaOH and increasing sodium acetate concentrations. The gradient was as follows: 0 to 140 mM (14 min), 140 to 300 mM (8 min), 300 to 400 mM (4 min), and then maintained at 500 mM (3 min). The column was re-equilibrated with 0.1 M NaOH for 4 min. The flow rate used was 0.4 mL/min, and the column temperature was maintained at 30°C. Signals were recorded by the amperometric detector and analyzed along with standard oligosaccharides of C1-C6 in length and their aldonic acids. The aldonic acid standard was prepared from corresponding native cello-oligosaccharides via selective C1 oxidation with Lugol's solution as described previously [14].

3. Results

3.1. Identification, codon optimization and synthesis of the MGG_00245 gene

Many carbohydrate-active enzymes are expressed by the rice fungal pathogen *M. oryzae* during appressorium development. The *MGG_00245* gene, which encodes a putative PMO, was identified by analyzing the published dataset obtained from transcriptional profiling of *M. oryzae* appressorium development [25]. The *MGG_00245* gene was found to be expressed during the early stages of appressorium formation, with a peak of expression at 16 h (Fig. 1). The protein encoded by the *MGG_00245* gene is a putative chitin-binding protein with characteristics of a polysaccharide monooxygenase.

Previous attempts to heterologously produce the *Mo*AA16 protein in *E. coli*, *Aspergillus*, and *Neurospora* were unsuccessful (data not shown). In this study, we therefore used *P. pastoris*, which is a commonly used host system for expressing heterologous proteins, along with codon optimization. Values such as Codon Adaptation Index (CAI), GC content, and Codon Frequency Distribution (CFD) can be used to optimize expression levels. CAI is calculated based on the distribution of the codon usage frequency along the length of the gene sequence and serves as a quantitative method of predicting the expression level of a gene [30]. An optimal CAI value of 1.0 is desired in the expression organism, while a CAI > 0.8 is considered desirable for gene expression levels. The CAI of the *MGG_00245* gene was improved from 0.6 to 0.93 after optimization. Following optimization, the GC content was adjusted from 62.2% to 41.3%, a value that still falls within the ideal range of 30-70%. Additionally, the CFD was significantly increased (Fig. S2). The optimized gene shared 61% nucleotide sequence identity with the native gene (Table S1, Fig. S1, Fig. S2, Fig. S3, Fig. S4).

The active site of PMOs features a motif known as the "*histidine brace*", which consists of two histidines [10]. This brace, comprising the N-terminal histidine (His1) and another histidine residue, serves as three equatorial ligands in coordination with copper ions [11,31]. Therefore, when expressing heterologous active PMOs, it is crucial to ensure the presence of the N-terminal histidine residue. This histidine is essential for proper copper coordination, and any absence or substitution with another amino acid would lead to protein inactivation [11,32]. Consequently, the selection or design of an appropriate secretory signal sequence becomes important. This signal sequence is responsible for the precise cleavage from the pre-protein, exposing the His1 residue, and ultimately contributing to the formation of an active PMO. SignalP prediction (https://services.healthtech.dtu.dk/services/SignalP-5.0/) indicated that *Mo*AA16 is likely a secreted protein with a 22-amino-acid signal peptide at the N-terminus (Fig. S5). To expose the first histidine, the cloning construct was designed to remove the native signal peptide (Fig. 2e).

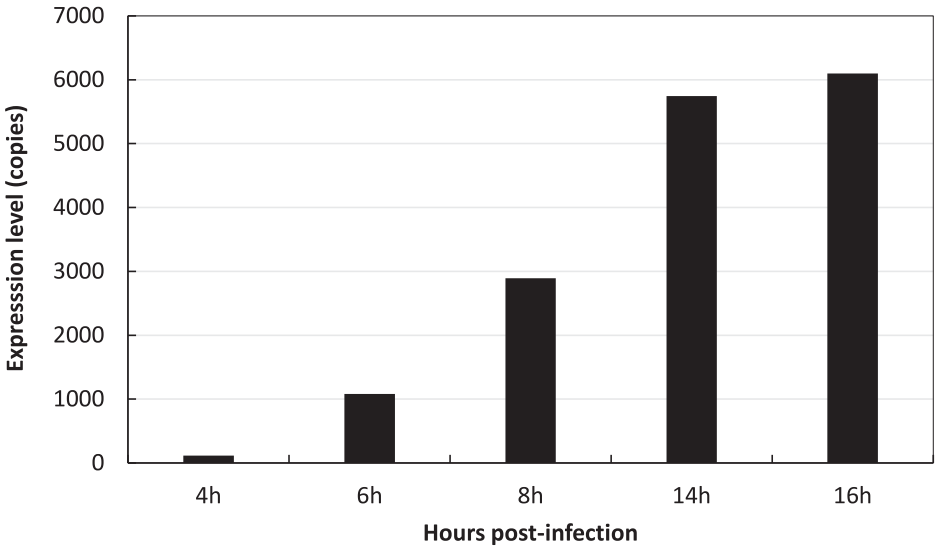

Fig. 1. The expression level of the MGG_00245 gene during appressorium development. Fungal spores were cultured on plastic coverslips to induce appressorium formation and incubated for up to 16 h (T16) [25].

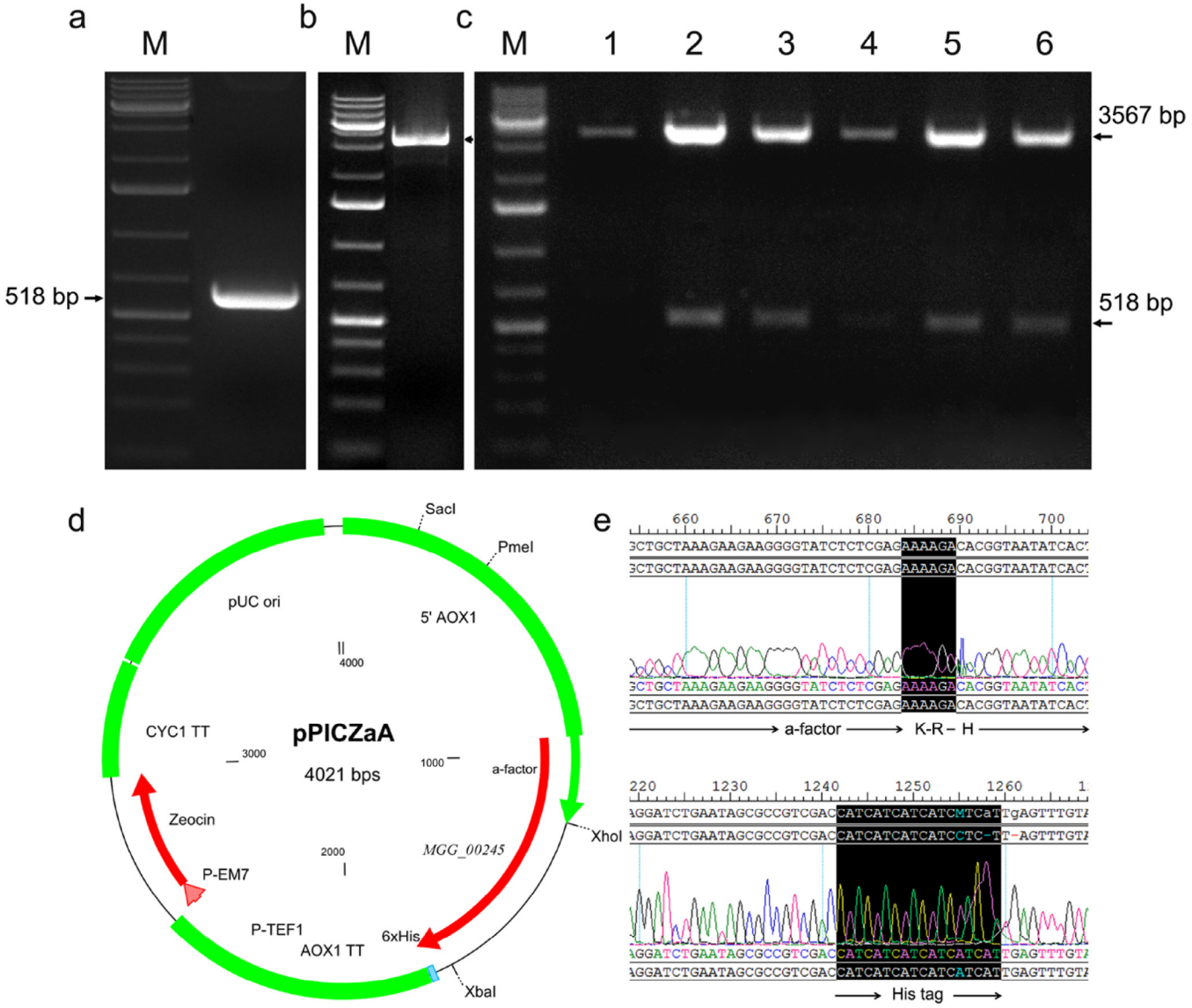

Fig. 2. Cloning of the *M. oryzae MGG_00245* gene into the pPICZαA vector. (a) Agarose gel image showing the PCR product of the *MGG_00245* gene (indicated by an arrow). (b) Agarose gel image illustrating the pPICZαA vector (indicated by an arrow). (c) Agarose gel image presenting the recombinant pPICZαA-*MGG_00245* vector and the inserted *MGG_00245* gene (indicated by an arrow), isolated from five *E. coli* colonies (lanes 1-6) and digested with *Xho*I and *Xba*I. M represents the GeneRuler 1 kb plus DNA ladder (Fermentas). (d) Diagrammatic map of the recombinant pPICZαA-*MGG_00245* vector (created using the Clone Manager Suite). (e) Partial sequence of the recombinant pPICZαA-*MGG_00245* vector showing the α-factor, the *MGG_00245* gene, and the His_6-tag (DNA star software).

3.2. Cloning and sequencing

A 518 bp fragment of the *M. oryzae MGG_00245* gene, excluding the amino-terminal signal peptide, was amplified using PCR with specific primers containing recognition sequences for restriction enzymes (Fig. 2a). Subsequently, the PCR amplicon was digested with the corresponding restriction enzymes and cloned into the pPICZαA vector under the control of the *P. pastoris AOX1* promoter, which is inducible with methanol. As depicted in Fig. 2e, the gene was cloned with an α-factor encoding the *P. pastoris* secretion signal at the 5́ end and a hexa histidine-tag encoding sequence at the 3́ end, facilitating protein purification through chromatography.

The recombinant pPICZαA-*MGG_00245* extracted from five *E. coli* transformed colonies was digested with *Xho*I and *Xba*I, resulting in the expected production of two bands: a 518 bp band (representing the gene of interest) and a 3,567 bp band (corresponding to the pPICZαA vector) (Fig. 2b, c). To confirm that the *MGG_00245* gene was in frame with the secretion signal sequence and the His-tag, a segment of the recombinant vector was sequenced using primers 5'AOX1-F and 3'AOX1-R (Fig. 2d). The linearized recombinant pPICZαA-*MGG_00245* vector was then transformed into *P. pastoris* X33 cells, and positive colonies were selected based on their resistance to Zeocin, a marker in the pPICZαA vector.

3.3. Small-scale protein expression and purification

To assess the expression levels of the *Mo*AA16-His-tag fusion protein, 24 positive *P. pastoris* transformed colonies were cultured in 2.5 mL BMGY medium in a Micro-24 plate. Subsequently, they were induced in 10 mL BMMY supplemented with 1% v/v methanol for 24, 48, and 72 h. After induction, the expression of the recombinant protein was confirmed by Western blot analysis in both the culture medium and cell lysate. The mature *Mo*AA16 protein con-

sists of 166 amino acids and has a calculated molecular mass of 17,591.24 Daltons. It was fused to His_6-tags in the pPICZαA vector, resulting in a calculated molecular mass of 20,326.21 Daltons. Immunoblot analysis revealed a distinct band of the expected size (approximately 20 kDa) in the intracellular fraction obtained from the majority of the transformed colonies (Fig. 3a). Additionally, a second band of approximately 40 kDa was also detected. NetNGlyc 1.0 (www.cbs.dtu.dk/services/NetNGlyc/) and NetOGlyc 4.0 (www.cbs.dtu.dk/services/NetOGlyc/) servers predicted four putative N-linked and one putative O-linked glycosylation sites, respectively, in the MGG_00245 amino acid sequence (Fig. S6, Fig. S7), indicating potential high N- and O-glycosylation levels, as seen in previous studies on PMOs. The recombinant protein was purified using its fused His_6-tag and eluted with up to 400 mM imidazole (lane 6, Fig. 3b).

3.4. Large-scale expression and purification

After separating the fermentation culture into ECF and ICF through centrifugation, the ECF was purified by tangential filtration and the ICF was broken down by ultrasonic treatment to obtain the target protein. The methanol/sorbitol-induced samples were compared to negative control samples without induction. The results of the SDS-PAGE analysis showed that there was no target protein observed in the ECF samples from both induced and control samples, while a 40 kDa protein band was observed in the induced ICF but not in the non-induced ICF. This indicates that the *Mo*AA16 protein was expressed in yeast cells with a size of 40 kDa but was not secreted (Fig. 4). The larger size of the protein obtained from *P. pastoris* is likely due to glycosylation after translation, as expected. Similar results were observed for other PMOs expressed in yeast or filamentous expression systems [1].

The intracellular fraction was further purified to obtain a large quantity of the target protein using a 20 × 100 mm Ni-NTA column based on the affinity binding between the hexahistidine tag and the Ni-NTA resin. The protein was eluted using a phosphate buffer with increasing imidazole concentration (30–250 mM). Fig. 5 shows the purified *Mo*AA16 protein with a molecular weight of 40 kDa. The eluted fractions (E2-E5) were collected for the next purification steps.

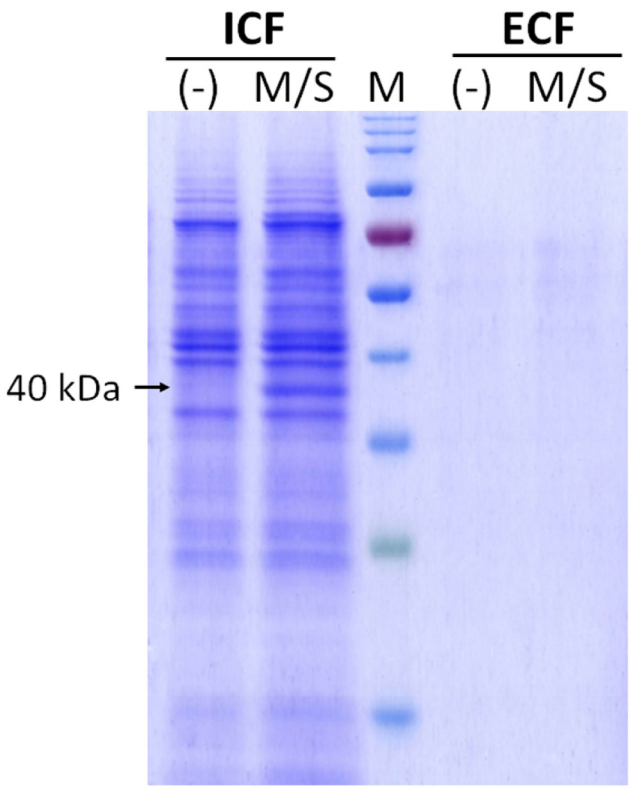

Fig. 4. Total proteins in the ECF and ICF of *P. pastoris* analyzed by SDS-PAGE. M/S: Sample from Methanol/Sorbitol-Induced Batch; (-): Sample from Non-Induced Batch; M: Protein Standard. Arrow indicates the target protein of about 40 kDa.

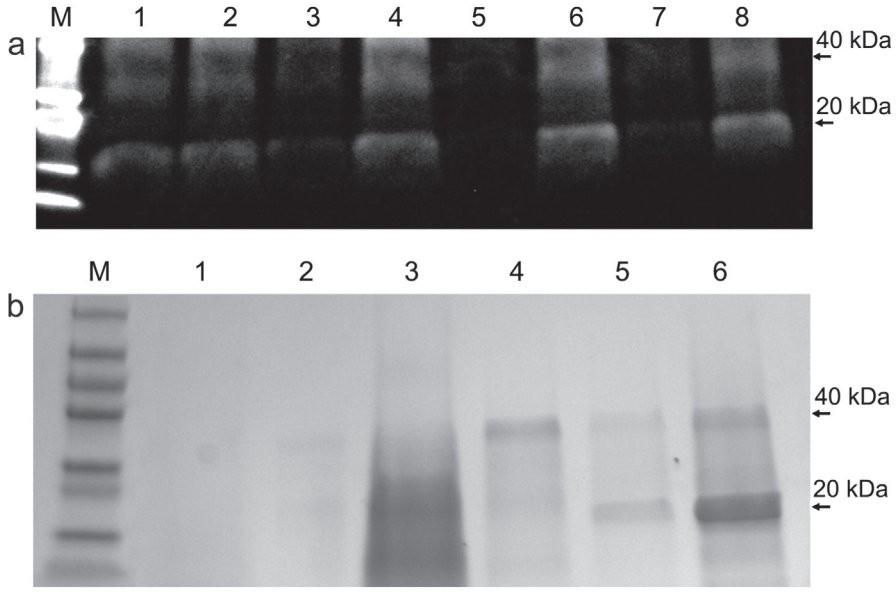

Fig. 3. Expression and purification of the *M. oryzae MoAA16*-His_6-tag fusion protein. (a) Western blot image depicting the expression level of the *Mo*AA16-His_6-tag fusion protein in ICF after 72 h of induction. Lanes 1-8 represent eight *P. pastoris* transformed colonies; M: Protomarker Protein Markers (National Diagnostics). The protein was probed using a 6×His monoclonal antibody (Serotec). (b) SDS-PAGE gel image showing the purification of the *Mo*AA16-His_6-tag fusion protein using nickel affinity chromatography. M: indicates the protein ladder; Lanes 1-2 correspond to the eluted fractions of non-induced *P. pastoris* colonies; Lane 3 is the flow-through; Lane 4 is the first wash with 20 mM imidazole; Lane 5 is the second wash with 40 mM imidazole; Lane 6 is the fraction eluted with 400 mM imidazole. The gel was visualized using instant blue staining.

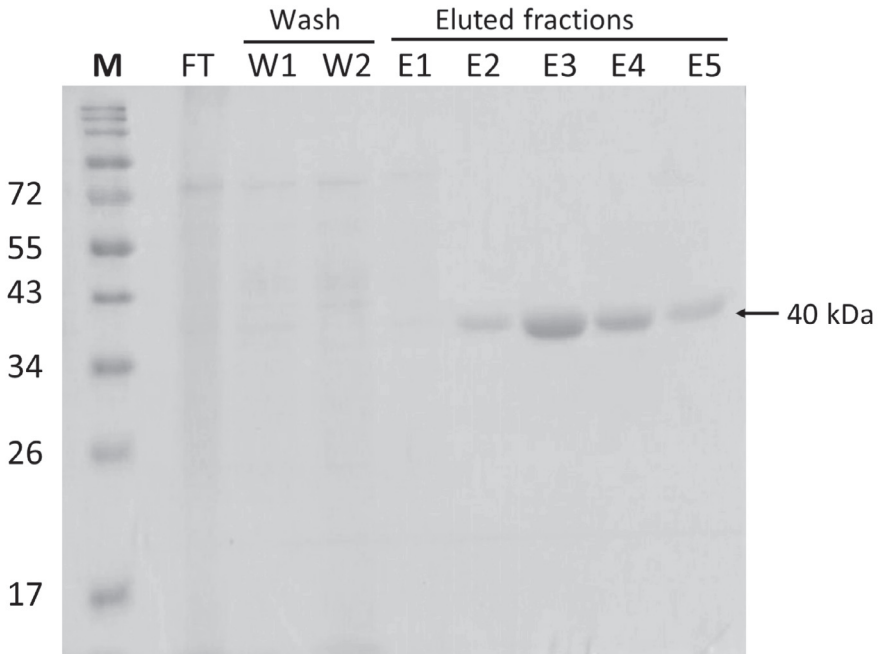

Fig. 5. SDS-PAGE gel of fractions obtained in the purification of *Mo*AA16 using Ni-NTA Column. M: Protein standard marker; FT: flow-through solution; W1-W2: column wash; E1-E5: target protein eluted fractions.

The protein fractions were collected using a MiniTrap™ G-25 PD column. They were then exchanged into 50 mM Tris-HCl buffer at pH 8.0, and the kex2 protease reaction was performed to remove the α-factor (Fig. 6a). The purified *Mo*AA16 protein was filtered using a Vivaspin 20 column with a 10 kDa molecular weight cut-off and confirmed by SDS-PAGE gel (Fig. 6b). The protein purity was 94%, as evaluated using ImageJ. The expression efficiency was calculated to be 66.76 mg/L, which is lower than some published results but still within the range reported in the literature (45 mg/L to over 300 mg/L depending on PMO classification) [33].

3.5. PMO activity

The determination of PMO catalytic activity is more challenging than that of glycoside hydrolases (GHs) enzymes due to the limited solubility of the oligo-aldonic acid/ketoaldose products. Indeed, the oxidation products remain considerably insoluble. The oxidizing capacity of PMO is proportional to the amount of oxidized insoluble polysaccharide substrate, but analyzing this substrate is still difficult [34]. To overcome this issue, the cellulose substrate used in the *in vitro* reaction was treated with phosphoric acid to

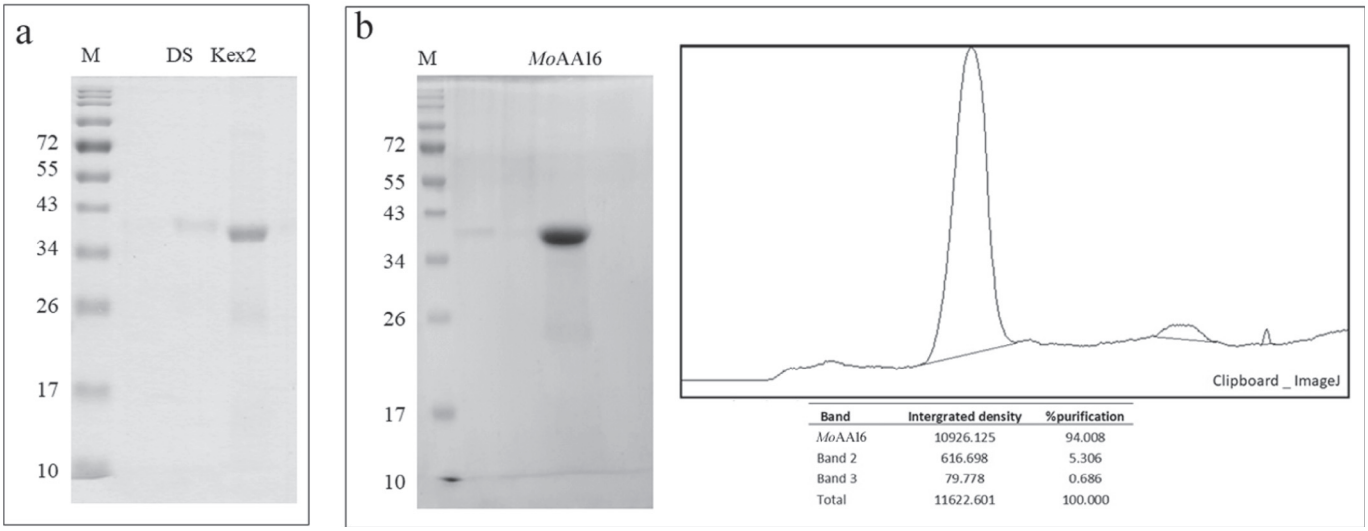

Fig. 6. Post-purification α-factor cleavage of the *Mo*AA16 protein. (a) SDS-PAGE analysis of the *Mo*AA16 protein after desalting (DS) and α-factor removal with kex2 protease; (b) SDS-PAGE analysis of the final purified protein. Percentage of purification was evaluated using ImageJ tool.

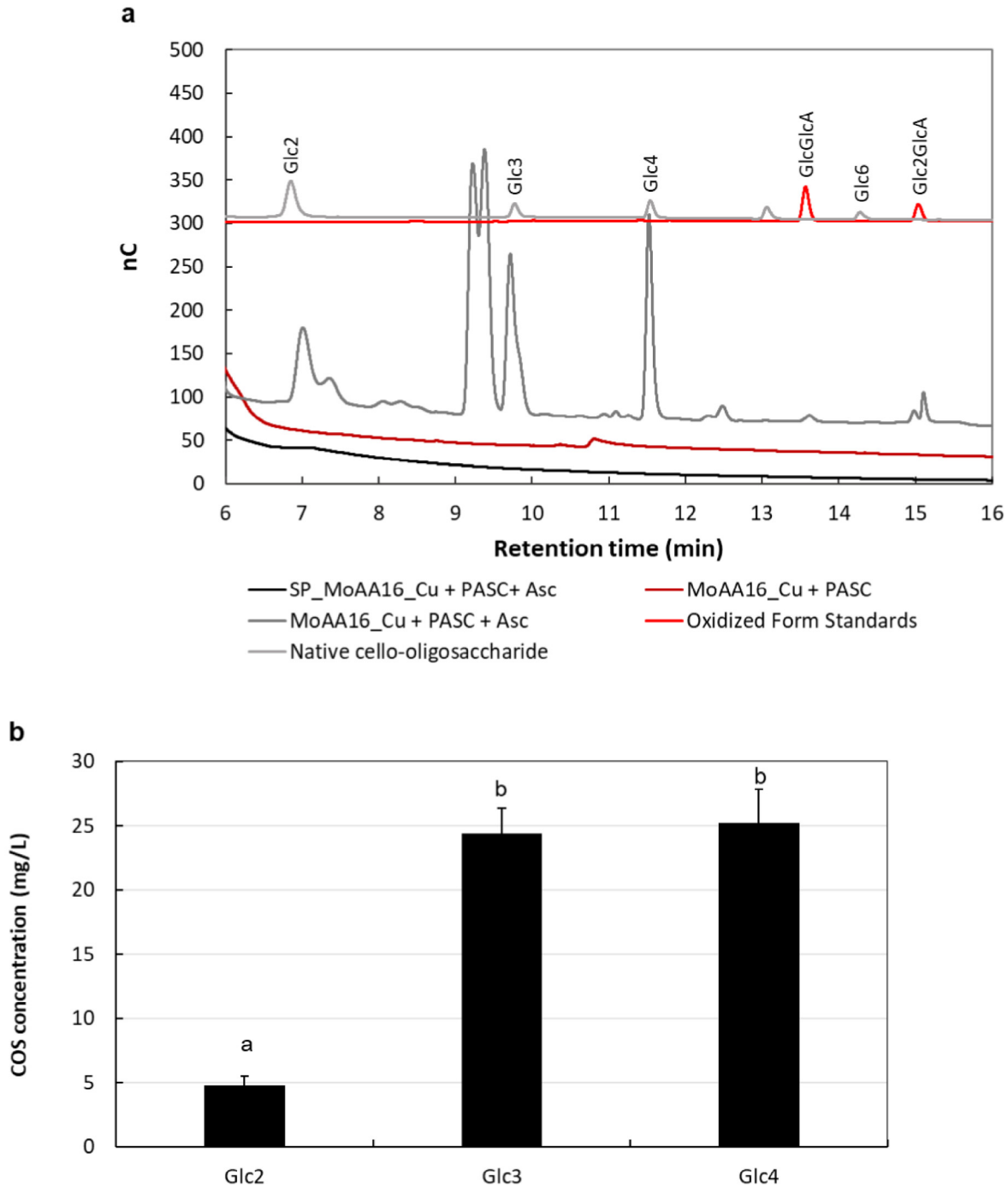

Fig. 7. Products of *Mo*AA16 reaction. (a) chromatogram and (b) concentrations of the products.

form PASC, which expands the structure of Avicel PH101 microcrystalline cellulose, promoting enzyme catalysis and making it easier to observe the products formed in the soluble phase. The HPAEC-PAD method is widely used to detect PMO activity and was applied to analyze the soluble oligosaccharide products produced by PMO in the reaction reported below. The balanced equations show general PMO reaction schemes for O_2-driven PMO activity. Two electrons from external sources are necessary to complete one catalytic cycle: the first one reduces Cu(II) to Cu(I), the second one reacts with Cu(I) and O_2 to form the PMO-Cu(II)-O* complex and oxidize the glycosidic bond of the substrate R-H [2,4,8,9,10,11].

$$\text{PMO-Cu(II)} + 1\ e^- \rightarrow \text{PMO-Cu(I)}$$

$$\text{PMO-Cu(I)} + 1\ e^- + O_2 + 2\ H^+ + \text{R-H} \rightarrow \text{PMO-Cu(II)} + H_2O + \text{R-OH}$$

The redox reaction of PMO is a crucial process in the cleavage of polysaccharides, including cellulose. In order to initiate the PMO reaction, several components are required: PMO-Cu(II), the substrate (in this case, PASC), an electron donor, and aerobic conditions. To study the PMO reaction, we conducted an experiment using the *Mo*AA16_Cu(II) enzyme, PASC substrate, ascorbic acid as the electron donor, and incubated the reaction at 42°C with 100 rpm shaking. The reaction was monitored for 16 h, and the

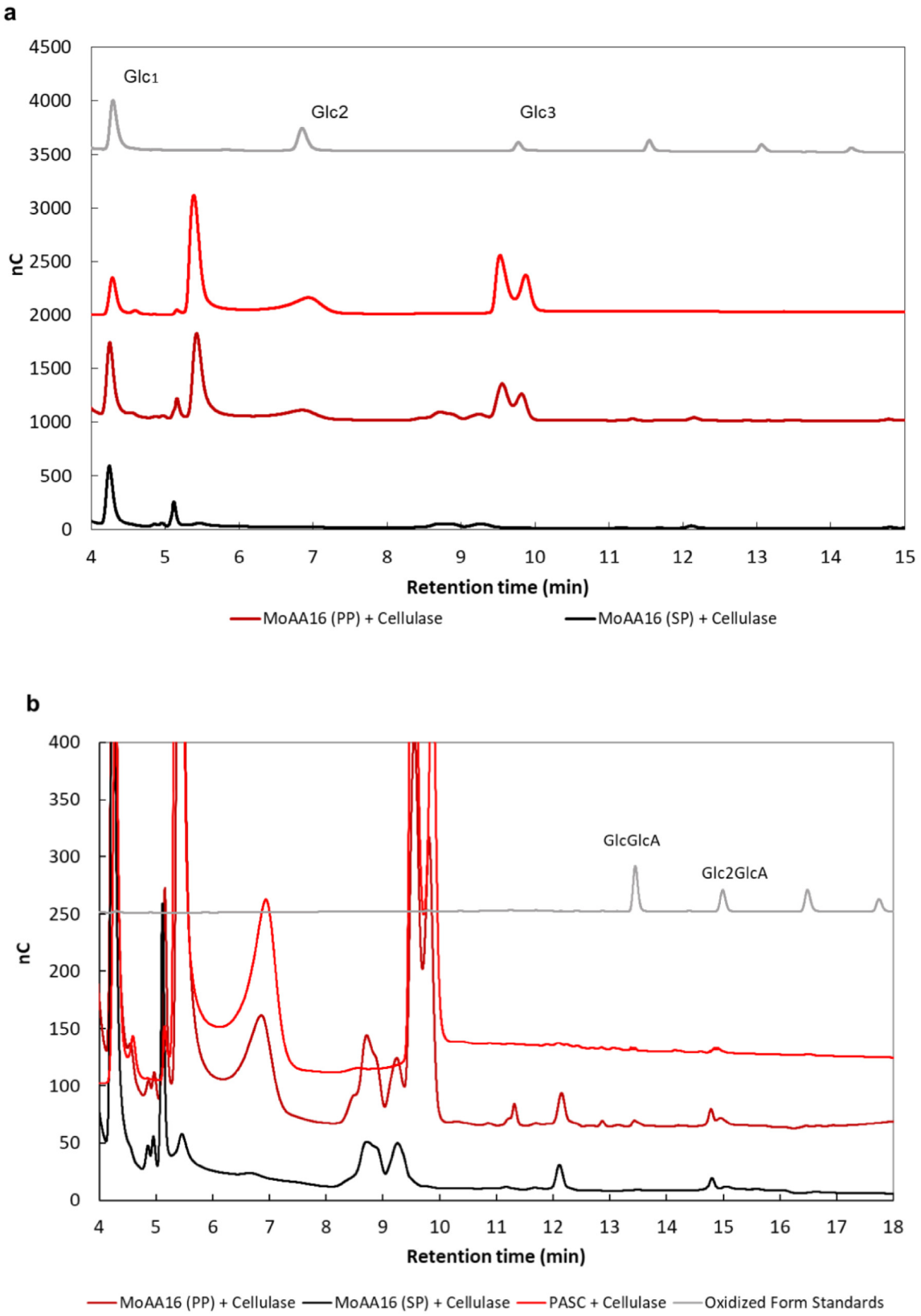

Fig. 8. The two-stage processing products of *Mo*AA16 and cellulase. (a) displays the primary cello-oligosaccharides Glc1 to Glc3; (b) demonstrates the presence of aldonic acids in the product (C1-ox product). (c) concentrations of Glc1 and Glc3 (mg/L). The characters show the significance of different statistical between groups when analyzing variance by ANOVA ($P \leq 0.05$); "*": significance between experimental groups; "a,b": significance between Glc groups.

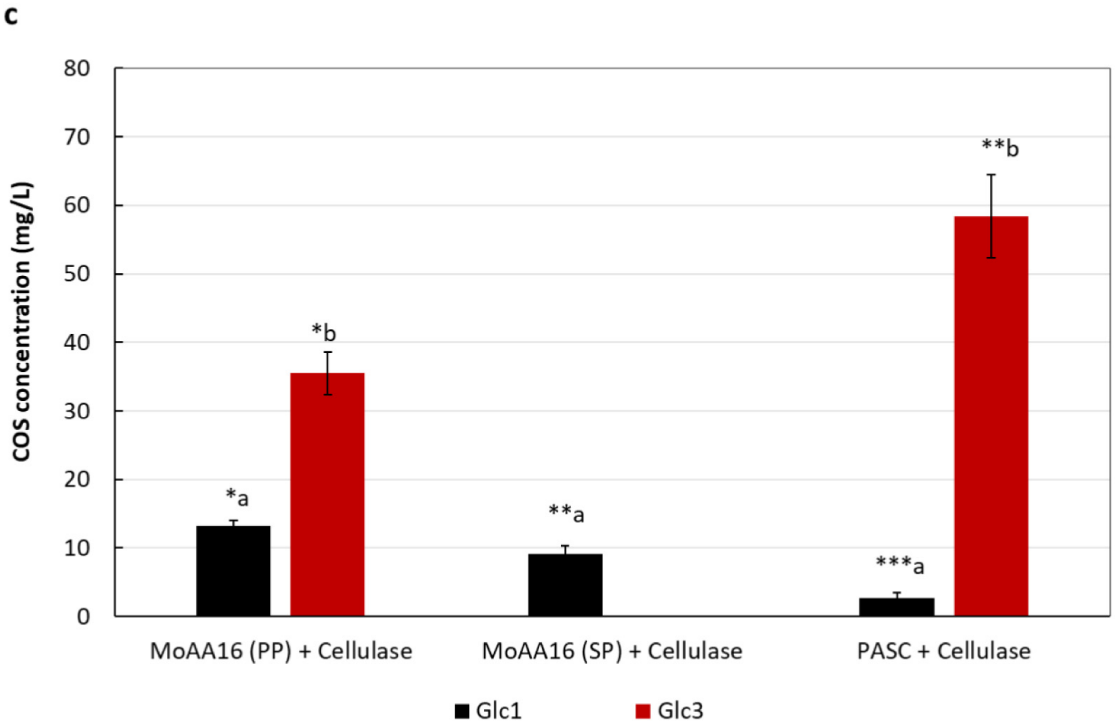

Fig. 8 (*continued*)

products were analyzed using HPAEC-PAD. The results showed that cellulose cleavage only occurred when ascorbic acid was present, acting as the electron donor (Fig. 7a). This experiment confirms that supplying electrons from an external source is necessary for the PMO reaction to occur, and the cleavage of the substrate is determined by the electron donor. Furthermore, when the reaction was performed with Kex2-untreated *Mo*AA16 (*Mo*AA16 with α-factor), no products were observed (Fig. 7a). This finding highlights the importance of correctly removing the signal peptide to expose the N-terminal His1, which plays a crucial role in PMO enzyme activity.

The products of the *Mo*AA16 reaction primarily consist of Glc2 - Glc4 oligosaccharides, represented by peaks of cellobiose (Glc2) with a retention time of 6.80 min, cellotriose (Glc3) at 9.73 min and cellotetraose (Glc4) at 11.65 min (Fig. 7). Additionally, the analysis showed the presence of small peaks corresponding to oxidized cellobionic acid (GlcGlc-A) at 13.44 min and cellotrionic acid (Glc2Glc-A) at 15 min). These correspond to the aldonic acid forms of cellotriose. This demonstrates that the *Mo*AA16 reaction cleaved the glycosidic bonds at the C1 position, creating intermediate lactone products that eventually hydrated into aldonic acids (Fig. 7). Furthermore, the same experiment was performed using a starch substrate (equivalent to maltodextrin 4.0–7.0). However, the results revealed no appearance of C1 oxidized products on the chromatogram (Fig. S8).

3.6. Two-stage reaction of PASC with PMO and cellulase

Both the soluble products (SP) and the remaining insoluble products (PP) obtained from the PMO activity were further treated with the cellulase enzyme and the reaction products were analyzed using HPAEC-PAD.

Fig. 8a,c illustrates the outcomes of the two-stage processing. Compared to the main products of the treatment with cellulase only (cello-oligosaccharides from Glc1 to Glc3, with cellotriose as the main product) in the samples first treated with *Mo*AA16, the main product was Glc1 in both the soluble (*Mo*AA16(SP)) and insoluble (*Mo*AA16(PP)) fractions. This indicates that processing with *Mo*AA16 enhances the cellulase hydrolysis reaction of the PASC substrate in producing more monosaccharide products. Additionally, in the two-stage processed samples, aldonic acids (C1-oxidized products) were present in small amounts (Fig. 8b).

3.7. One-stage reaction of PASC with PMO and cellulase

The one-stage reaction of recombinant *Mo*AA16 and cellulase with the PASC substrate was performed with the aim of demonstrating the synergistic effect of the two enzymes. The results of the HPAEC-PAD analysis indicated that when only cellulase was used to process PASC, the reaction resulted in 5 types of oligosaccharides (Glc1 to Glc5) (Fig. 9). However, when *Mo*AA16 and cellulase were both added to the reaction, only 4 types of oligosaccharides (Glc1 to Glc4) were produced, with a higher amount of mono-, di-, and tri-saccharide (Fig. 9). This result demonstrated that *Mo*AA16 enhances the catalytic ability of cellulase to produce a greater amount of short-chain carbohydrates. Additionally, the synergistic effect provided by *Mo*AA16 over time was investigated by analyzing the amount of cellotriose produced. The results showed that the presence of *Mo*AA16 increased the amount of cellotriose produced compared to cellulase alone, and the enhancing effect occurred in the first 1-3 h of the reaction (Fig. 10).

4. Discussion

PMOs are important enzymes involved in breaking down recalcitrant polysaccharides such as cellulose, making them crucial in a variety of industrial and biotechnological applications. Unfortunately, many PMOs cannot be expressed in commonly used *E. coli* expression systems. An alternative expression system is

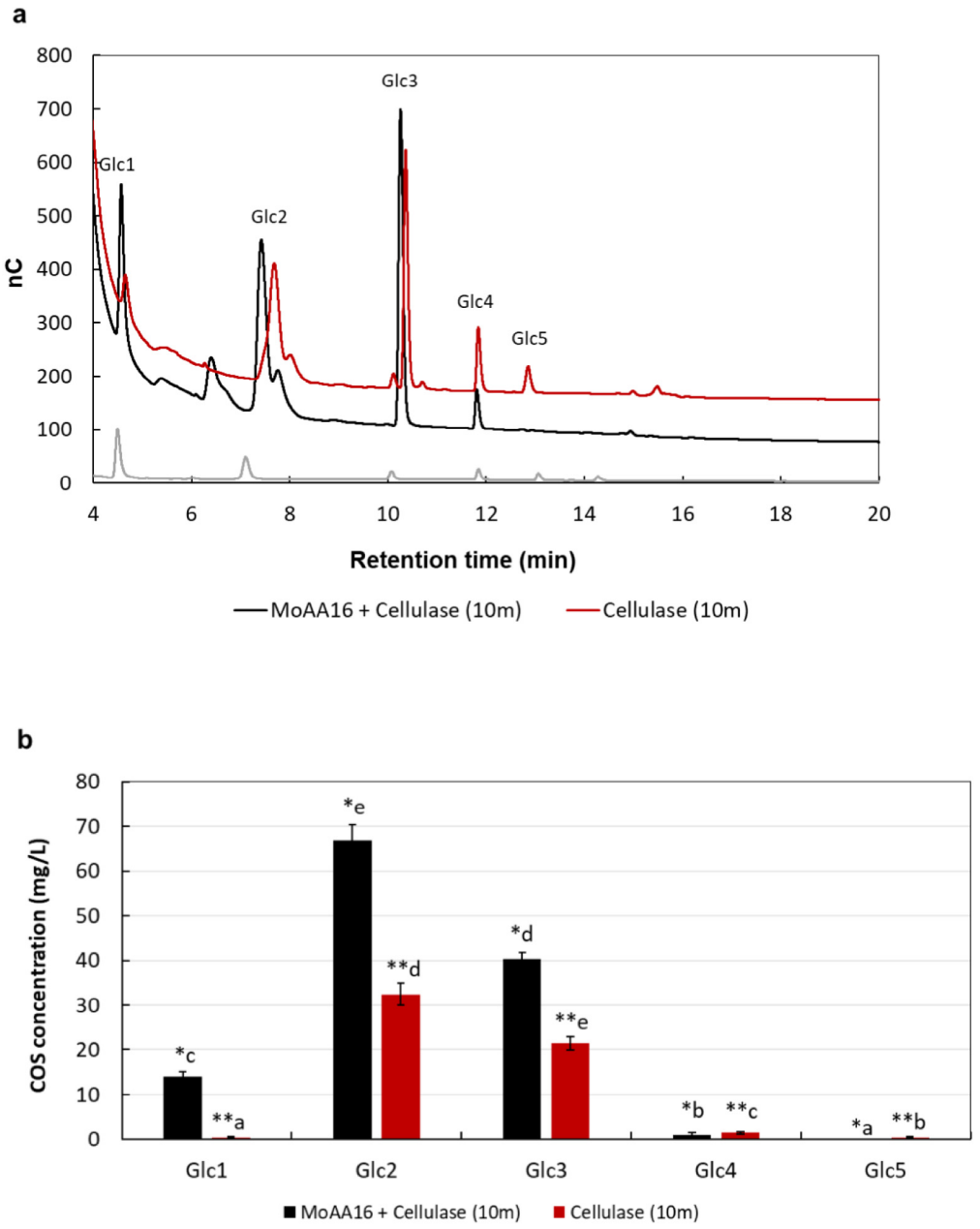

Fig. 9. The one-stage processing products of *Mo*AA16 and cellulase after 10 min of reaction. (a) chromatogram and (b) concentrations of the products. The characters show the significance of different statistical between groups when analyzing variance ANOVA ($P \leq 0.05$); "*": significance between experiment groups; "a,b,c,d,e": significance between Glc groups.

the yeast *Pichia pastoris*. This is due to its efficient and cost-effective production capabilities, as well as its ability to produce large amounts of high-quality proteins. Numerous studies have demonstrated the ability of *P. pastoris* to produce various PMOs [33,35]. Despite its many advantages, *P. pastoris* has some limitations for PMO production. One of these limitations is its inability to perform methylation of the amino-terminal histidine found in fungal PMOs. However, it does have the ability to glycosylate proteins, which have been shown to play an important role in ensuring the correct folding of PMOs from eukaryotic organisms [36]. Indeed, glycosylation can affect their folding, stability, and activity. To obtain an active PMO through heterologous expression, the following features were important: (i) an appropriate signal peptide for correct processing and secretion; (ii) no amino-terminal tag to preserve the His residue in position 1, the α-amino group and side-chain are crucial for copper binding and catalysis; (iii) proper copper saturation; (iv) suitable glycosylation and methylation for expression and stability; and (v) codon optimization for improved expression level [37,38]. The most widely used vector for PMO production in *P. pastoris* is the commercially available pPICZα vector (Invitrogen) [15,33]. This vector is convenient as it allows cloning to be performed in *E. coli* before being introduced into *P. pastoris* for protein expression. The vector also contains signal sequences useful for protein secretion.

The *MGG_00245* gene of the rice fungal pathogen *M. oryzae* is highly expressed during plant infection and particularly during appressorium development [25] and encodes a putative chitin-binding protein with characteristics of a PMO (*in silico* analysis).

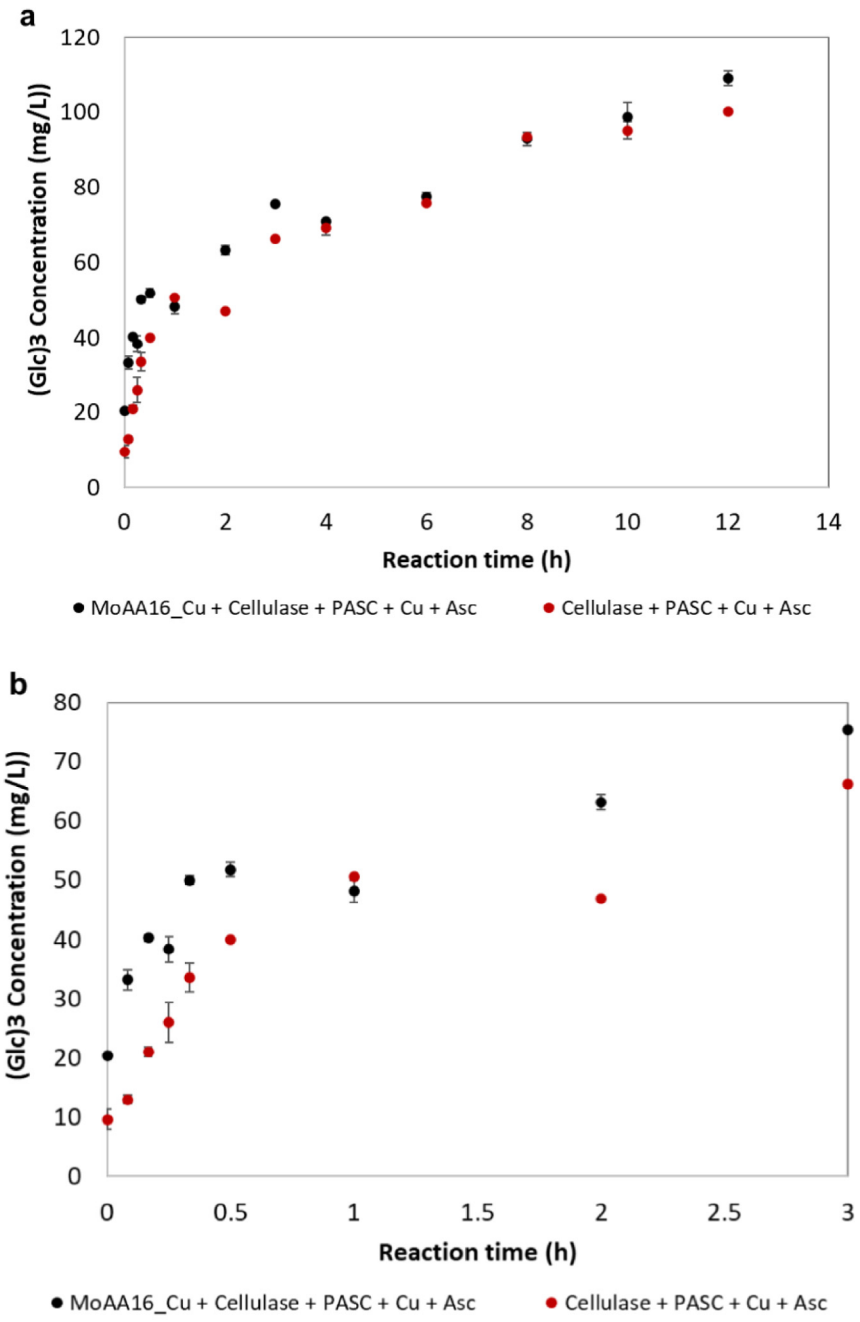

Fig. 10. Peak area for cellotriose (Glc3) produced in the reaction over time. PMO_Cu + cellulase; cellulase. Reaction time: 12 h (a) and 3 h (b).

This study provides a simple and fast protocol for cloning, expressing, and purifying this PMO. The protocol has been designed to include all the steps needed for the purification and characterization of the final product. To increase expression levels of the gene in *P. pastoris*, codon optimization was performed by adjusting the Codon Adaptation Index (CAI), GC content, and Codon Frequency Distribution (CFD). One important feature of PMOs is that their active site is coordinated by the histidine "brace" and the histidine in position 1 is critical for coordinating copper ions and maintaining protein activity. From the literature, it is reported that obtaining functional PMO proteins is difficult due to self-oxidation of the recombinant enzyme. In particular, a common problem is the oxidation and/or substitution of the amino-terminal histidine with other amino acids [38]. By removing the native signal peptide at the amino-terminus of *Mo*AA16 and by cloning the amino-terminal histidine after the cleavage site of the *P. pastoris* signal peptide, we were able to produce a functional recombinant protein in this heterologous system.

The expression level of the *Mo*AA16-hexahistidine tagged fusion protein was tested by culturing 24 positive transformed colonies of *P. pastoris* and inducing them with methanol. The expression of the recombinant protein was verified by Western blot. Unexpectedly, the recombinant protein was detected only intracellularly. A possible explanation for the lack of secretion could be the poor stability of the protein once the signal peptide has been removed. Further investigations are needed to clarify this

unexpected result. In the intracellular fraction of *P. pastoris*, we detected the expected band of 20 kDa and an additional band of 40 kDa. Since the *Mo*AA16 protein has several putative N-linked and O-linked glycosylation sites, a high level of glycosylation by *P. pastoris* probably resulted in an increase in the molecular weight of the recombinant protein. Previous studies have shown that PMO proteins, when heterologously expressed using the *P. pastoris* system, are readily N- and/or O-glycosylated, leading to a higher-than-expected protein size [1].

Interestingly, in the subsequent large-scale expression experiment we detected only the 40 kDa recombinant protein. The only difference between the large and small-scale experiments that could explain this result is the type of feeding strategy used for induction, with methanol/sorbitol and PTM1 being used for the large-scale expression. This trace element may be responsible for protein self-assembly to form dimers or higher oligomeric aggregates [39]. For example, Radford and coworkers have shown that the addition of metal ions such as Ni^{2+}, Co^{2+}, Cu^{2+}, and Zn^{2+} (which are components of PTM1) induces cytochrome cb562 dimerization, leading to an increase in the overall stability of the protein. Zn ions are also exploited as strong metal ions for protein synthesis in homodimers [40]. The metal ions are attached at the interface of the protein and form metal bridges leading to molecular assembly into functional aggregates (dimers, modifiers, or higher oligomeric). Although to date, there have not been any published PMOs expressed as dimers, but this is also a hypothesis worthy of attention. The binding of metal ions to hook peptides needs to be evaluated by different methods (NMR, ITC, MS, UV-vis, and circular dichroism spectroscopy). In this study, the 40 kDa recombinant protein was therefore purified using nickel affinity chromatography and eluted with imidazole. The purified protein was evaluated using SDS-PAGE gel image analysis software, revealing a purity of 94% and an expression efficiency of about 66 mg/L medium. This yield is lower than some published results but falls within the reported range in the literature. Kittl et al. [33] expressed four PMO coding genes from *Neurospora crassa* in *P. pastoris* and obtained products with yields ranging from 45 to 300 mg/L. Rieder et al. [41] also used *P. pastoris* platform for the expression of four different PMOs spanning three different families, the yield reaching up to 42 mg/L of pure PMO.

The recombinant *Mo*AA16 was then tested for its ability to oxidize cellulose in the presence of ascorbic acid as an electron donor. Determining the activity of the PMO enzyme is challenging compared to other GH enzymes. The oxidation products produced after PMO catalysis remain considerably insoluble, making them difficult to analyze. To overcome this, the cellulose substrate used in the *in vitro* reaction was treated with phosphoric acid to form PASC, which expands the structure of the substrate and makes it easier to observe the soluble phase products. The HPAEC-PAD method was used to detect *Mo*AA16 activity and analyze the soluble oligosaccharide products produced. The redox reaction of PMO requires PMO-Cu(II), substrate, electron donor, and aerobic conditions. In an experiment with the *Mo*AA16 enzyme, PASC substrate, and ascorbic acid as the electron donor, cellulose cleavage only occurred in the presence of ascorbic acid, demonstrating its important role as an electron donor. These findings improve our understanding of the PMO reaction and its potential role in the degradation of plant cellulose, which is crucial in many industrial and biological processes.

The *Mo*AA16 reaction mainly produced Glc2-Glc4 oligosaccharides and cellobionic and cellotrionic acids. *Mo*AA16 functioned as a depolymerizing enzyme with a copper redox center, breaking down glycosidic bonds at the C1 position. This is in accordance with the descriptions of Filiatrault-Chastel et al. [1] on the new AA16 PMO enzyme. Indeed, based on its amino acid sequence similarity to AA16, the presence of two conserved histidines and its cellulose degradation ability, the *Mo*AA16 protein can be considered a cellulose-active PMO of the rice blast fungus *M. oryzae* and could be therefore renamed *Mo*AA16. *Mo*AA16 was also previously annotated as a chitin-binding type-4 domain-containing protein. It is now shown to have cellulose-active PMO activity. Cellulose and chitin are similar in structure; they are both made from glucose monomers and form microfibrils that are tightly bound together by hydrogen bonds. However, cellulose and chitin are different polysaccharides with distinct chemical properties. Cellulose possesses a hydroxyl group on the C2 carbon, while chitin has an acetamide group. In certain instances, the interaction between the chitin-binding domain and substrates, whether chitin or cellulose, can be attributed to the connection between aromatic residues in the enzyme and the pyranose ring of the polysaccharide. The side chains present on the polysaccharide have a limited impact on this binding. Consequently, some chitin-binding domains exhibit similar binding affinities for both chitin and cellulose [42].

In this study, experiments were also conducted to analyze the effect on cellulose hydrolysis of adding *Mo*AA16 to the cellulase enzyme. Results from HPAEC-PAD analysis showed that the presence of the *Mo*AA16 protein in the reaction mixture enhanced the hydrolysis efficiency of cellulase, resulting in the production of more monosaccharides and oligosaccharides with a higher amount of cellobiose and cellotriose compared to a reaction with cellulase alone.

PMO families are found across a wide range of pathogens, including fungi, oomycetes, bacteria, and viruses. The association between PMOs and pathogenic processes has garnered significant attention, with numerous studies demonstrating their crucial role in polysaccharide cleavage within the cortical layer and their involvement in host penetration. In a study by Vandhana et al. [43], the authors emphasized the significant functions of PMOs in fungal and oomycete plant pathogenesis, such as potato late blight, as well as in mutualistic and commensal symbiotic relationships like ectomycorrhizae. They also delved into the potential relevance of PMOs in different forms of microbial pathogenesis, including bacterial diseases such as pneumonia, fungal infections like human meningitis, oomycete-related disorders, and viral infections such as entomopox. Additionally, they explored the involvement of PMOs in the development of various (micro)organisms, including several plant pests.

For instance, *Pi*AA17 from *Phytophthora infestans* has been identified as a participant in host infection [44]. Similarly, *Pa*AA10 from *Pseudomonas aeruginosa*, a bacterial pathogen in humans, has been shown to promote systemic infection [45]. Additionally, *Aa*AA15 from *Aphanomyces astaci* has been found to play an essential role in interactions between animals and pathogens [46]. The CAZy database indicates that sequences encoding AA16 family PMOs are also present in numerous plant pathogens such as the blast fungus *M. oryzae*, the early wheat blight fungus *Fusarium graminearum*, the gray mold fungus *Botrytis cinerea*, and the leaf spot disease-causing fungus *Curvularia clavate*, among others. Gene regulation analysis has revealed increased expression of *Mo*AA16 and other carbohydrate-metabolizing enzymes during the development of the infectious structure known as the appressorium. This finding supports the hypothesis that the *Mo*AA16 enzyme actively contributes to the development of blast symptoms. However, further experiments are necessary to fully validate this hypothesis. The relationship between PMOs and pathogenesis is an area of active research, and continued investigations will provide a deeper understanding of their roles in the disease-causing processes of various pathogens. Furthermore, we utilized MobiDB-lite 3.0 and the IUPred2A algorithm to analyze the amino acid sequence of *Mo*AA16. The findings revealed the presence of a LDR, SEEDLNSALD, which aligns with previous research by Tamburrini et al.

[29]. However, additional investigations are required to elucidate the significance of this LDR in terms of cellulose degradation activity or the pathogenicity of the blast fungus *M. oryzae*.

5. Conclusions

In the present study, a new polysaccharide monooxygenase (PMO) from the fungus *M. oryzae* (*Mo*AA16, coded by the gene *MGG_00245*), the causal agent of the rice blast disease, was heterologously expressed in the methylotrophic yeast *P. pastoris* and the recombinant protein was purified and characterized enzymatically. *Mo*AA16 is able to cleave the glycosidic bond of cellulose at the C1 position through oxidative cleavage, facilitated by the presence of a copper ion in its active site. This result provides the first experimental evidence of the PMO catalytic activity of *Mo*AA16. The presence of the *Mo*AA16 protein in the reaction mixture enhanced the hydrolysis efficiency of cellulose on a cellulose substrate, increasing the production of monosaccharides. This new PMO could be an interesting tool to improve the degradation of cellulose in many industrial and biotechnological applications.

Author contributions

- Study conception and design: HM Nguyen, VV Vu, L Sella, RM Bill.
- Data collection: HM Nguyen, LQ Le, VV Vu, LM Broadbent.
- Analysis and interpretation of results: HM Nguyen, LQ Le, VV Vu.
- Draft manuscript preparation: HM Nguyen, VV Vu, L Sella, LQ Le, RM Bill.
- Revision of the results and approval of the final version of the manuscript: HM Nguyen, VV Vu, LQ Le.

Financial support

This work is part of the Scientific and Technological Cooperation Agreement between the Ministry of Science and Technology of Vietnam and the Italian Ministry of Foreign Affairs and International Cooperation (grant No. NĐT.36.ITA/18). We also acknowledge the UK Biotechnology and Biological Sciences Research Council through the Global Challenges Research Fund Project, CAPRI-BIO (BB/P022685/1).

Conflicts of interest

The authors declare no conflict of interest.

Data availability

All Data and Materials are present in the main paper.

Supplementary material

Supplementary data to this article can be found online at https://doi.org/10.1016/j.ejbt.2023.06.002.

References

[1] Filiatrault-Chastel C, Navarro D, Haon M, et al. AA16, a new lytic polysaccharide monooxygenase family identified in fungal secretomes. Biotechnol Biofuels 2019;12:55. https://doi.org/10.1186/s13068-019-1394-y. PMid: 30923563.
[2] Arfi Y, Shamshoum M, Rogachev I, et al. Integration of bacterial lytic polysaccharide monooxygenases into designer cellulosomes promotes enhanced cellulose degradation. PNAS 2014;111(25):9109–14. https://doi.org/10.1073/pnas.1404148111. PMid: 24927597.
[3] Forsberg Z, Mackenzie AK, Sørlie M, et al. Structural and functional characterization of a conserved pair of bacterial cellulose-oxidizing lytic polysaccharide monooxygenases. PNAS 2014;111(23):8446–51. https://doi.org/10.1073/pnas.1402771111. PMid: 24912171.
[4] Vaaje-Kolstad G, Westereng B, Horn SJ, et al. An oxidative enzyme boosting the enzymatic conversion of recalcitrant polysaccharides. Science 2010;330 (6001):219–22. https://doi.org/10.1126/science.1192231. PMid: 20929773.
[5] Hemsworth GR, Henrissat B, Davies GJ, et al. Discovery and characterization of a new family of lytic polysaccharide monooxygenases. Nat Chem Biol 2014;10:122–6. https://doi.org/10.1038/nchembio.1417. PMid: 24362702.
[6] Lo Leggio L, Simmons TJ, Poulsen JCN, et al. Structure and boosting activity of a starch-degrading lytic polysaccharide monooxygenase. Nat Commun 2015;6:5961. https://doi.org/10.1038/ncomms6961. PMid: 25608804.
[7] Vu VV, Beeson WT, Span EA, et al. A family of starch-active polysaccharide monooxygenases. PNAS 2014;111(38):13822–7. https://doi.org/10.1073/pnas.1408090111. PMid: 25201969.
[8] Phillips CM, Beeson WT, Cate JH, et al. Cellobiose dehydrogenase and a copper-dependent polysaccharide monooxygenase potentiate cellulose degradation by *Neurospora crassa*. ACS Chem Biol 2011;6(12):1399–406. https://doi.org/10.1021/cb200351y. PMid: 22004347.
[9] Forsberg Z, Vaaje-Kolstad G, Westereng B, et al. Cleavage of cellulose by a CBM33 protein. Protein Sci 2011;20(9):1479–83. https://doi.org/10.1002/pro.689. PMid: 21748815.
[10] Westereng B, Ishida T, Vaaje-Kolstad G, et al. The putative endoglucanase pcGH61D from *Phanerochaete chrysosporium* is a metal-dependent oxidative enzyme that cleaves cellulose. PLoS ONE 2011;6(11):e27807. https://doi.org/10.1371/journal.pone.0027807. PMid: 22132148.
[11] Quinlan RJ, Sweeney MD, Lo Leggio L, et al. Insights into the oxidative degradation of cellulose by a copper metalloenzyme that exploits biomass components. PNAS 2011;108(37):15079–84. https://doi.org/10.1073/pnas.1105776108. PMid: 21876164.
[12] Harris PV, Welner D, McFarland KC, et al. Stimulation of lignocellulosic biomass hydrolysis by proteins of glycoside hydrolase family 61: Structure and function of a large, enigmatic family. Biochemistry 2010;49(15):3305–16. https://doi.org/10.1021/bi100009p. PMid: 20230050.
[13] Arora R, Bharval P, Sarswati S, et al. Structural dynamics of lytic polysaccharide monoxygenases reveals a highly flexible substrate binding region. J Mol Graph Model 2019;88:1–10. https://doi.org/10.1016/j.jmgm.2018.12.012. PMid: 30612037.
[14] Beeson WT, Phillips CM, Cate JHDD, et al. Oxidative cleavage of cellulose by fungal copper-dependent polysaccharide monooxygenases. JACS 2012;134 (2):890–2. https://doi.org/10.1021/ja210657t. PMid: 22188218.
[15] Couturier M, Ladevèze S, Sulzenbacher G, et al. Lytic xylan oxidases from wood-decay fungi unlock biomass degradation. Nat Chem Biol 2018;14:306–10. https://doi.org/10.1038/nchembio.2558. PMid: 29377002.
[16] Sabbadin F, Hemsworth GR, Ciano L, et al. An ancient family of lytic polysaccharide monooxygenases with roles in arthropod development and biomass digestion. Nat Commun 2018;9:756. https://doi.org/10.1038/s41467-018-03142-x. PMid: 29472725.
[17] Horn SJ, Vaaje-Kolstad G, Westereng B, et al. Novel enzymes for the degradation of cellulose. Biotechnol Biofuels 2012;5:45. https://doi.org/10.1186/1754-6834-5-45. PMid: 22747961.
[18] Hemsworth GR, Davies GJ, Walton PH. Recent insights into copper-containing lytic polysaccharide mono-oxygenases. COSB 2013;23(5):660–8. https://doi.org/10.1016/j.sbi.2013.05.006. PMid: 23769965.
[19] Yakovlev I, Vaaje-Kolstad G, Hietala AM, et al. Substrate-specific transcription of the enigmatic GH61 family of the pathogenic white-rot fungus *Heterobasidion irregulare* during growth on lignocellulose. Appl Microbiol Biotechnol 2012;95:979–90. https://doi.org/10.1007/s00253-012-4206-x. PMid: 22718248.
[20] Beeson WT, Vu VV, Span EA, et al. Cellulose degradation by polysaccharide monooxygenases. Annu Rev Biochem 2015;84:923–46. https://doi.org/10.1146/annurev-biochem-060614-034439. PMid: 25784051.
[21] Yan X, Talbot NJ. Investigating the cell biology of plant infection by the rice blast fungus *Magnaporthe oryzae*. Curr Opin Microbiol 2016;34:147–53. https://doi.org/10.1016/j.mib.2016.10.001. PMid: 27816794.
[22] Nalley L, Tsiboe F, Durand-Morat A, et al. Economic and environmental impact of rice blast pathogen (*Magnaporthe oryzae*) alleviation in the United States. PLoS One 2016;11(12):e0167295. https://doi.org/10.1371/journal.pone.0167295. PMid: 27907101.
[23] Oses-Ruiz M, Sakulkoo W, Littlejohn GR, et al. Two independent S-phase checkpoints regulate appressorium-mediated plant infection by the rice blast fungus *Magnaporthe oryzae*. PNAS 2017;114(2):E237–44. https://doi.org/10.1073/pnas.1611307114. PMid: 28028232.
[24] Dagdas YF, Yoshino K, Dagdas G, et al. Septin-mediated plant cell invasion by the rice blast fungus, *Magnaporthe oryzae*. Science 2012;336(6088):1590–5. https://doi.org/10.1126/science.1222934. PMid: 22723425.
[25] Soanes DM, Chakrabarti A, Paszkiewicz KH, et al. Genome-wide transcriptional profiling of appressorium development by the rice blast fungus *Magnaporthe oryzae*. PLoS Pathogens 2012;8(2):e1002514. https://doi.org/10.1371/journal.ppat.1002514. PMid: 22346750.
[26] Žifčáková L, Baldrian P. Fungal polysaccharide monooxygenases: New players in the decomposition of cellulose. Fungal Ecol 2012;5(5):481–9. https://doi.org/10.1016/j.funeco.2012.05.001.
[27] Jenkinson CB, Jones K, Zhu J, et al. The appressorium of the rice blast fungus *Magnaporthe oryzae* remains mitotically active during post-penetration hyphal

growth. Fungal Genet Biol 2017;98:35–8. https://doi.org/10.1016/j.fgb.2016.11.006. PMid: 27890626.
[28] Sun P, Huang Z, Banerjee S, et al. AA16 Oxidoreductases boost cellulose-active AA9 lytic polysaccharide monooxygenases from *Myceliophthora thermophila*. ACS Catal 2023;13(7):4454–67. https://doi.org/10.1021/acscatal.3c00874. PMid: 37066045.
[29] Tamburrini KC, Terrapon N, Lombard V, et al. Bioinformatic analysis of lytic polysaccharide monooxygenases reveal the pan-families occurrence of intrinsically disordered C-terminal extensions. Biomolecules 2021;11 (11):1632. https://doi.org/10.3390/biom11111632. PMid: 34827630.
[30] Sharp PM, Li WH. The codon adaptation index-a measure of directional synonymous codon usage bias, and its potential applications. Nucl Acids Res 1987;15(3):1281–95. https://doi.org/10.1093/nar/15.3.1281. PMid: 3547335.
[31] Vu VV, Beeson WT, Phillips CM, et al. Determinants of regioselective hydroxylation in the fungal polysaccharide monooxygenases. JACS 2014;136 (2):562–5. https://doi.org/10.1021/ja409384b. PMid: 24350607.
[32] Li X, Beeson IV WT, Phillips CM, et al. Structural basis for substrate targeting and catalysis by fungal polysaccharide monooxygenases. Structure 2012;20 (6):1051–61. https://doi.org/10.1016/j.str.2012.04.002. PMid: 22578542.
[33] Kittl R, Kracher D, Burgstaller D, et al. Production of four *Neurospora crassa* lytic polysaccharide monooxygenases in *Pichia pastoris* monitored by a fluorimetric assay. Biotechnol Biofuels 2012;5:79. https://doi.org/10.1186/1754-6834-5-79. PMid: 23102010.
[34] Wang D, Li Y, Zheng Y, et al. Recent advances in screening methods for the functional investigation of lytic polysaccharide monooxygenases. Front Chem 2021;9:653754. https://doi.org/10.3389/fchem.2021.653754. PMid: 33912540.
[35] Tanghe M, Danneels B, Camattari A, et al. Recombinant expression of *Trichoderma reesei* Cel61A in *Pichia pastoris*: optimizing yield and n-terminal processing. Mol Biotechnol 2015;57:1010–7. https://doi.org/10.1007/s12033-015-9887-9. PMid: 26285758.
[36] Karbalaei M, Rezaee SA. *Pichia pastoris*: A highly successful expression system for optimal synthesis of heterologous proteins. Cell Physiol 2020;235 (9):5867–81. https://doi.org/10.1002/jcp.29583. PMid: 32057111.
[37] Eijsink VGH, Petrovic D, Forsberg Z, et al. On the functional characterization of lytic polysaccharide monooxygenases (LPMOs). Biotechnol Biofuels 2019;12:58. https://doi.org/10.1186/s13068-019-1392-0. PMid: 30923566.
[38] Petrović DM, Bissaro B, Chylenski P, et al. Methylation of the N-terminal histidine protects a lytic polysaccharide monooxygenase from auto-oxidative inactivation. Protein Sci 2018;27(9):1636–50. https://doi.org/10.1002/pro.3451. PMid: 29971843.
[39] Dang DT. Molecular approaches to protein dimerization: Opportunities for supramolecular chemistry. Front Chem 2022;10:829312. https://doi.org/10.3389/fchem.2022.829312. PMid: 35211456.
[40] Brodin JD, Medina-Morales A, Ni T, et al. Evolution of metal selectivity in templated protein interfaces. JACS 2010;132(25):8610–7. https://doi.org/10.1021/ja910844n. PMid: 20515031.
[41] Rieder L, Ebner K, Glieder A, et al. Novel molecular biological tools for the efficient expression of fungal lytic polysaccharide monooxygenases in *Pichia pastoris*. Biotechnol Biofuels 2021;14:122. https://doi.org/10.1186/s13068-021-01971-5. PMid: 34044872.
[42] Kikkawa Y, Fukuda M, Kashiwada A, et al. Binding ability of chitinase onto cellulose: an atomic force microscopy study. Polym J 2011;43:742–4. https://doi.org/10.1038/pj.2011.60.
[43] Vandhana TM, Reyre JL, Sushmaa D, et al. On the expansion of biological functions of lytic polysaccharide monooxygenases. New Phytol 2022;233 (6):2380–96. https://doi.org/10.1111/nph.17921. PMid: 34918344.
[44] Sabbadin F, Urresti S, Henrissat B, et al. Secreted pectin monooxygenases drive plant infection by pathogenic oomycetes. Science 2021;373(6556):774–9. https://doi.org/10.1126/science.abj1342. PMid: 34385392.
[45] Askarian F, Uchiyama S, Masson H, et al. The lytic polysaccharide monooxygenase CbpD promotes *Pseudomonas aeruginosa* virulence in systemic infection. Nat Commun 2021;12:1230. https://doi.org/10.1038/s41467-021-21473-0. PMid: 33623002.
[46] Sabbadin F, Henrissat B, Bruce NC, et al. Lytic polysaccharide monooxygenases as chitin-specific virulence factors in crayfish plague. Biomolecules 2021;11 (8):1180. https://doi.org/10.3390/biom11081180. PMid: 34439846.